Journal of Alloys and Compounds 507 (2010) 547–550

Contents lists available at ScienceDirect

Journal of Alloys and Compounds

journal homepage: www.elsevier.com/locate/jallcom

Anomalous hydrogen absorption on non-stoichiometric iron-carbon compound

Hiroki Miyaoka [a], Takayuki Ichikawa [a,b,*], Tatsuo Fujii [c], Wataru Ishida [b], Shigehito Isobe [a], Hironobu Fuji [a,b], Yoshitsugu Kojima [a,b]

[a] Institute for Advanced Materials Research, Hiroshima University, 1-3-1 Kagamiyama, Higashi-Hiroshima, Hiroshima 739-8530, Japan
[b] Department of Quantum Matter, ADSM, Hiroshima University, 1-3-1 Kagamiyama, Higashi-Hiroshima, Hiroshima 739-8530, Japan
[c] Department of Applied Chemistry, Okayama University, 3-1-1 Tsushima-naka, Okayama, Okayama 700-8530, Japan

ARTICLE INFO

Article history:
Received 15 June 2010
Received in revised form 29 July 2010
Accepted 30 July 2010
Available online 11 August 2010

Keywords:
Hydrogen absorbing materials
Amorphous materials
Mechanochemical processing
Mössbauer spectroscopy
X-ray and gamma-ray spectroscopies
Thermal analysis

ABSTRACT

On the synthesis of nano-structural hydrogenated graphite by ball-milling under H_2 atmosphere, iron contamination was mingled from steel balls during ball-milling. It is clarified by spectroscopic measurements that the mingled iron formed a non-stoichiometric iron–carbon (Fe–C) compound. The Fe–C phase was transformed to a well-ordered phase with H_2 desorption at 450 °C, suggesting that the hydrogen atoms were anomalously trapped at the Fe–C phase. With respect to hydrogen absorbing properties, the mingled iron enhanced the hydrogen capacity by about 50% compared with iron free hydrogenated graphite, where H/Fe was about 13 mass%. Therefore, if the hydrogen absorption site originated in the Fe–C phase could be synthesized independently, it should be recognized as a promising hydrogen storage system.

1. Introduction

In 1999, it was reported that the hydrogenated nano-structural graphite ($C^{nano}H_x$) can store the large amount hydrogen due to the chemisorptions [1]. So far, the hydrogen absorption and desorption properties on $C^{nano}H_x$ have been investigated by various experimental methods, thermal analysis and structural examination [2–7], neutron scattering measurements [8,9], infra-red absorption spectroscopy [10], nuclear magnetic resonance spectroscopy [11,12], electron energy-loss spectroscopy with transmission electron microscope [13–15], and electron spin resonance spectroscopy [16].

$C^{nano}H_x$ was synthesized from graphite by ball-milling using steel balls under H_2 atmosphere for 80 h [1]. Regarding the hydrogen absorption state, it was reported by Fukunaga et al. [8], Itoh et al. [9], and Ogita et al. [10] that the hydrogen atoms were chemisorbed as stable hydrocarbon groups. Thus, the hydrogen absorption sites are the electronic active graphene edges and defects induced by the formation of nano-structure during ball-milling [16], where it is named C–H site in this paper. On the other hand, Isobe et al. reported that a considerable amount of iron was mingled into $C^{nano}H_x$ from "steel balls" during the ball-milling, resulting that the higher hydrogen capacity was obtained [4]. Therefore, it is expected that the iron in $C^{nano}H_x$ forms the other hydrogen absorption site.

In this paper, two types of $C^{nano}H_x$ were synthesized by ball-milling using steel balls and ZrO_2 balls in order to understand the iron effect for hydrogen absorption and desorption properties. For the products, various kinds of experimental analyses were performed. From the results, the iron effect on the hydrogen absorption and desorption properties of $C^{nano}H_x$ was discussed.

2. Experimental technique

2.1. Sample preparation

To synthesize $C^{nano}H_x$, Graphite powder (99.999%, Stream Chemicals) of 300 mg were put into a milling vessel made of Cr steel (SKD-11, Umetoku Co. Ltd.), which is inner volume of 30 cm^3, with 20 steel (SUJ-2) balls with 7 mm diameter or 20 ZrO_2 balls with 8 mm diameter. The ball-milling was performed under 1 MPa of H_2 pressure for 80 h at room temperature by using a planetary (rotating) ball-mill apparatus (P7, Fritsch). All the samples were handled in a glove-box (MP-P60W, Miwa MFG) filled with purified Ar gas (>99.9999%) to avoid an oxidation. $C^{nano}H_x$ synthesized by using the "steel" balls and the "ZrO_2" balls are respectively named $C^{nano}H_x$ (steel) and $C^{nano}H_x$ (ZrO_2).

2.2. Experimental procedure

The hydrogen desorption properties of $C^{nano}H_x$ (steel) and $C^{nano}H_x$ (ZrO_2) were examined by a thermal desorption mass spectroscopy (TDMS, M-QA200TS, Anelva). TDMS equipment is installed inside the glove-box to minimize an influence of the

* Corresponding author at: Institute for Advanced Materials Research, Hiroshima University, 1-3-1 Kagamiyama, Higashi-Hiroshima, Hiroshima 739-8530, Japan. Tel.: +81 (0) 82 424 5744; fax: +81 (0) 82 424 5744.
E-mail address: tichi@hiroshima-u.ac.jp (T. Ichikawa).

0925-8388/$ – see front matter © 2010 Elsevier B.V. All rights reserved.
doi:10.1016/j.jallcom.2010.07.221

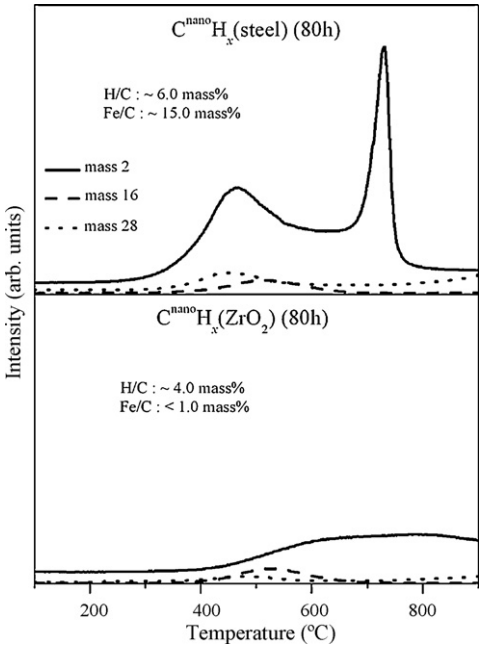

Fig. 1. Thermal desorption mass spectra of $C^{nano}H_x$ (steel) and $C^{nano}H_x$ (ZrO_2), in which mass 2, 16, and 28 correspond to H_2, CH_4, and C_2H_6, respectively.

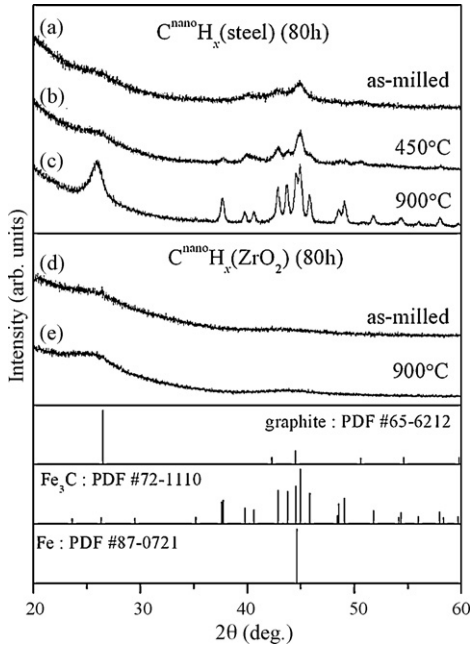

Fig. 2. XRD profiles of (a) $C^{nano}H_x$ (steel) product after synthesizing, (b) annealing at 450 °C for 8 h, (c) heating up to 900 °C, (d) $C^{nano}H_x$ (ZrO_2) after synthesizing, and (e) heating up to 900 °C. The XRD profiles of graphite (PDF #65-6212), Fe_3C (PDF #72-1110), and Fe (PDF #87-0721) are referred from database.

oxidation and the water adsorption on the samples. In TDMS, high-purity helium (He) gas (>99.9999%) was flowed as a carrier gas, and the heating rate was fixed at 10 °C/min. Some kinds of fragments near expected desorption gases, H_2, CH_4, and C_2H_6, were monitored in TDMS to assign the desorption gases.

In order to estimate the hydrogen and iron amount in the products, elemental analysis was carried out by using oxygen-combustion method (2400α CHN analyzer, Perkin-Elmer) with a high-purity oxygen gas (>99.9999%). For the elemental analysis, all the samples of about 2 mg were covered by tin (Sn) foil in the glove-box. By using this analysis, each amount of C and H in the samples was accurately measured. A residue corresponding to the iron amount can be evaluated by a subtraction of the C and H amount from the total sample amount because $C^{nano}H_x$ was mainly composed of C and H atoms.

The structural change was investigated by an X-ray diffraction (XRD) measurement (RINT-2100: Cu Kα radiation, Rigaku). For the XRD measurements, in order to avoid an oxidation during the XRD measurements, all the samples were covered by a polyimide sheet (Kapton®, Du Pont-Toray Co. Ltd.) in the glove-box.

The chemical state of iron in $C^{nano}H_x$ (steel) was examined by Fe *K*-edge X-ray absorption spectroscopy (XAS) at BL19B2 beam-line of SPring-8 synchrotron radiation facility in Japan. The Fe *K*-edge X-ray absorption near edge structure (XANES) spectra of the as-synthesized and dehydrogenated $C^{nano}H_x$ (steel) were obtained in a transmission mode. As references, metallic iron (Fe^{foil}) (99.85%, 10 μm), iron carbide (Fe_3C) (99.9%, Rare Metallic), iron (II) chloride ($FeCl_2$) (99.998%, Aldrich), and iron oxy-hydroxide (FeOOH) were also measured. The samples were diluted by lithium hydroxide (LiOH) powder (98%, Aldrich) and formed as a pellet of 1 cm in diameter. After that, the samples were protected by the polyimide sheet to avoid the exposing the samples in air during the measurements.

Mössbauer spectroscopy of ^{57}Fe was carried out to characterize the iron-related phases in $C^{nano}H_x$ (steel) before and after H_2 desorption. ^{57}Co was used as the Mössbauer source. The sample of about 100 mg was formed as pellet of 1 cm in diameter and covered with the polyimide sheet in the glove-box to protect the samples from an oxidation during the measurements.

3. Results and discussion

The H_2 desorption properties of both the $C^{nano}H_x$ products were quite different as shown in Fig. 1. $C^{nano}H_x$ (steel) desorbs H_2 with characteristic two-peaks with heating, where each peak temperature was 450 and 700 °C, while the H_2 desorption from $C^{nano}H_x$ (ZrO_2) revealed a broad-peak in the wide temperature range from 400 to more than 900 °C. The hydrogen amount of $C^{nano}H_x$ (steel) was estimated to be H/C = 6 mass%, which was much larger than $C^{nano}H_x$ (ZrO_2), 4 mass%. The iron amount Fe/C in $C^{nano}H_x$ (steel) and $C^{nano}H_x$ (ZrO_2) was 15 mass% and less than 1 mass%, respectively. These results suggest that the hydrogen capacity of the ball-milled graphite is enhanced due to the iron contamination from milling balls. Under the above assumption, the hydrogen capacity for iron can be estimated to be H/Fe = 13 mass%, which was obtained from division of the excess hydrogen H/C = 2 mass% by the iron amount Fe/C = 15 mass%. This hydrogen capacity was relatively larger than the conventional hydrogen storage materials.

As shown in Fig. 2, the structural change with H_2 desorption of $C^{nano}H_x$ (steel) was clearly different from $C^{nano}H_x$ (ZrO_2). After ball-milling, diffraction peaks of graphite completely disappeared for both products, indicating that graphite structure was destroyed down to nano-meter size. In the XRD pattern of the as-milled $C^{nano}H_x$ (steel), quite broad peaks were observed, and these peaks might be ascribed to Fe_3C or Fe. After the first H_2 desorption of $C^{nano}H_x$ (steel) at 450 °C, broad diffraction peaks corresponding to Fe_3C appeared, indicating that a crystallization of Fe_3C was simul-

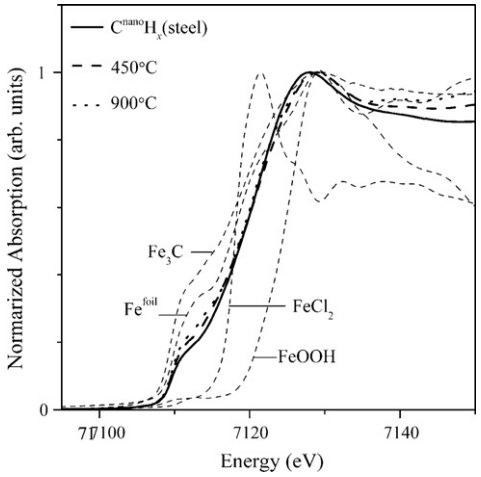

Fig. 3. Fe *K*-edge XANES spectra of $C^{nano}H_x$ (steel) after synthesizing (thick solid line), annealing at 450 °C for 8 h (thick dash line), and heating up to 900 °C (thick dot line). Thin dash lines represent XANES spectra of reference, Fe^{foil}, Fe_3C, $FeCl_2$, and FeOOH.

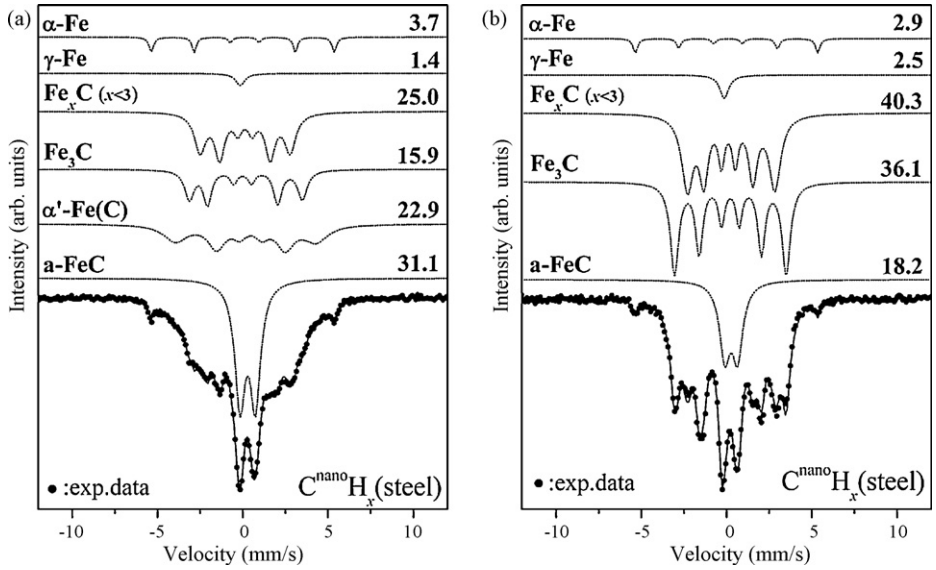

Fig. 4. Mössbauer spectra of (a) the as-synthesized $C^{nano}H_x$ (steel) after milling and (b) after annealing at 450 °C for 8 h. Dot lines represent the reference spectra obtained by database for fitting the experimental data, where α-Fe, γ-Fe, $Fe_xC(x<3)$, Fe_3C, α′-Fe(C), and a-FeC correspond to alpha-phase of iron, gamma-phase of iron, carbon-rich iron carbide, iron carbide, martensite steel, and amorphous Fe–C compound, respectively. Solid line is obtained as a sum of the fitting spectra. The number inserted on each fitting spectrum shows abundance ratio in the product.

taneously occurred with the H_2 desorption. The peaks assigned to Fe_3C were grown and the diffraction peak assigned to (0 0 2) plane of graphite appeared after the second H_2 desorption by the heating up to 900 °C. Differently, $C^{nano}H_x$ (ZrO_2) showed no peaks in the XRD patterns before and after H_2 desorption by heating up to 900 °C. A catalytic effect of iron for a graphitization has been investigating [17–19]. Recently, Huo et al. reported on a carbon-encapsulated iron nano-particle [20]. In this paper, it was clarified that the disordered carbon around iron particles was transformed to the well-ordered graphite structure by heat treatment at 1000 °C. The above results indicate that the 1st H_2 desorption at 450 °C of $C^{nano}H_x$ (steel) is strongly related to the structural transformation of the iron containing phase. Furthermore, the graphitization around the iron containing phase at 700 °C would accelerate the H_2 desorption from C–H site although the hydrogen of C–H site should be desorbed without graphitization.

In order to examine the chemical states of Fe in $C^{nano}H_x$ (steel), X-ray absorption spectroscopy (XAS) for Fe *K*-edge was carried out. The X-ray absorption near edge structure (XANES) spectra of the products are shown as thick lines in Fig. 3, where thick solid, dash, and dot lines show the spectra of this product after milling, annealing at 450 °C, and heating up to 900 °C, respectively. The onset of X-ray absorption for all the products was located at almost the same energy 7107 eV, which was close to Fe^{foil} and Fe_3C. The pre-edge-like structure in the region from 7110 to 7115 eV was also similar to Fe^{foil} and Fe_3C even though the normalized intensity was different. The pre-edge structure indicates that the electron density of state related to the hybridization between the *p* and *d* orbital in the Fe atoms exists around Fermi energy, suggesting that the electronic structure of the Fe in the product possesses metallic state differently from $FeCl_2$ and FeOOH. The normalized intensity of the pre-edge structure was changed to become higher with increase in the temperature, indicating that electronic structure was changed. From this result, it is expected that the change of electronic structure would be related to the H_2 desorption, assuming that the hydrogen atoms are trapped in the iron containing phase. Tatsumi et al. reported on the Fe *K*-edge XAS of hydrogenated nano-structural graphite [14]. They suggest the relation between the spectral change and hydrogen absorbed on the surface of iron by first principle calculations. Here, when the iron containing phase is composed of more than 2 phases (not single phase), the XANES spectrum should include the contribution from all the phases. Therefore, it should be clarified whether this spectral change is affected by the plural iron containing phases or not.

In order to identify the iron containing phases in further detail, the Mössbauer spectroscopy was carried out for $C^{nano}H_x$ (steel). The Mössbauer spectrum of the as-milled product is shown in Fig. 4(a). The phases with a higher abundance ratio were $Fe_xC(x<3)$, α′-Fe(C), and a-FeC, indicating that the iron containing phase in the product would be a non-stoichiometric Fe–C compound like amorphous. Fig. 4(b) shows the Mössbauer spectrum of $C^{nano}H_x$ (steel) after the annealing at 450 °C for 8 h. Noteworthy, the α′-Fe(C) phase completely disappeared and the abundance ratio of a-FeC obviously decreased. These spectral changes indicate that the formation of the Fe_3C and $Fe_xC(x<3)$ phases are occurred by the annealing at 450 °C, in other words, the iron containing phase was changed from non-stoichiometric Fe–C compound to well-ordered Fe_3C. This phenomenon was consistent with the structural change due to the 1st H_2 desorption. These results suggest that the hydrogen atoms are trapped around the grain boundary, vacancy, or carbon atoms in the non-stoichiometric Fe–C compound, which is named "Fe–C–H site". Then, the containing hydrogen is released with the structural transformation into Fe_3C. Actually, Takai et al. reported that hydrogen can be trapped at the strained interface between ferrite and Fe_3C and/or the interface dislocation enclosed between Fe_3C lamellae in cold-drawn high strength steel, and then the trapped hydrogen was desorbed at around 400 °C [21].

4. Conclusion

In this work, the iron effects for the hydrogen absorption/desorption properties of $C^{nano}H_x$ were characterized. The hydrogen capacity was enhanced from 4 to 6 mass% in the case of $C^{nano}H_x$ (steel) because this product possessed not only C–H site but also Fe–C–H site, which was the non-stoichiometric Fe–C compound with the characteristic electronic structure differently from metallic Fe. The characteristic two-peak H_2 desorption of $C^{nano}H_x$ (steel) was due to the iron effect. With increase in a temperature, the hydrogen trapped in Fe–C–H site was desorbed at 450 °C as first H_2 desorption by the structural transformation from

the non-stoichiometric Fe–C compound to the well-ordered Fe_3C. Simultaneously, the hydrogen desorption from C–H site should independently start at 400 °C, resulting that the H_2 desorption from both the sites should be overlapped in the temperature range from 400 to 650 °C. The 2nd H_2 desorption was almost finished at around 750 °C even though the H_2 desorption from C–H site should be continued above 900 °C. With respect to the second H_2 desorption of $C^{nano}H_x$ (steel), it is expected that the H_2 desorption from C–H site, which is hydrogen absorption site at the graphene edges and defects, is strongly accelerated due to the graphitization around Fe or Fe_3C particles. From above experimental facts, it is concluded that the anomalous hydrogen absorption state caused by the non-stoichiometric Fe–C compound coexist with the C–H site in the ball-milled graphite. Its hydrogen capacity is estimated to be H/(Fe–C–H) > 10 mass%, which is very larger value compared with conventional hydrogen storage materials. Therefore, if the Fe–C–H site could be isolated from the main carbon phase, it should be thought as a promising hydrogen storage system.

Acknowledgements

This work was supported by the project "Advanced Fundamental Research Project on Hydrogen Storage Materials" of the New Energy and Industrial Technology Development Organization (NEDO), Research Fellowships of the Japan Society for the Promotion of Science for young Scientists (JSPS), and the Sasakawa Scientific Research Grant from The Japan Science Society. The authors gratefully acknowledge Dr. Tetsuo Honma for valuable help of X-ray absorption spectroscopy at SPring-8 BL19B2, and Dr. Tsumuraya, Dr. Biswajit Paik for the good discussion and valuable help in this work.

References

[1] S. Orimo, G. Majer, T. Fukunaga, A. Züttel, L. Schlapbach, H. Fujii, Appl. Phys. Lett. 75 (1999) 3093–3095.
[2] S. Orimo, T. Matsushima, H. Fujii, T. Fukunaga, G. Majer, J. Appl. Phys. 90 (2001) 1545–1549.
[3] D.M. Chen, T. Ichikawa, H. Fujii, N. Ogita, M. Udagawa, Y. Kitano, E. Tanabe, J. Alloys Compd. 354 (2003) L5–L9.
[4] S. Isobe, T. Ichikawa, J.I. Gottwald, E. Gomibuchi, H. Fujii, J. Phys. Chem. Sol. 65 (2004) 535–539.
[5] T. Ichikawa, D.M. Chen, S. Isobe, E. Gomibuchi, H. Fujii, Mater. Sci. Eng. B: Solid State Mater. Adv. Technol. 108 (2004) 138–142.
[6] T. Kiyobayashi, K. Komiyama, N. Takeichi, H. Tanaka, H. Senoh, H.T. Takeshita, N. Kuriyama, Mater. Sci. Eng. B: Solid State Mater. Adv. Technol. 108 (2004) 134–137.
[7] E. Gomibuchi, T. Ichikawa, K. Kimura, S. Isobe, K. Nabeta, H. Fujii, Carbon 44 (2006) 983–988.
[8] T. Fukunaga, K. Itoh, S. Orimo, K. Aoki, Mater. Sci. Eng. B: Solid State Mater. Adv. Technol. 108 (2004) 105–113.
[9] K. Itoh, Y. Miyahara, S. Orimo, H. Fujii, T. Kamiyama, T. Fukunaga, J. Alloys Compd. 356 (2003) 608–611.
[10] N. Ogita, K. Yamamoto, C. Hayashi, T. Matsushima, S. Orimo, T. Ichikawa, H. Fujii, M. Udagawa, J. Phys. Soc. Jpn. 73 (2004) 553–555.
[11] G. Majer, E. Stanik, S. Orimo, J. Alloys Compd. 356 (2003) 617–621.
[12] E. Stanik, G. Majer, S. Orimo, T. Ichikawa, H. Fujii, J. Appl. Phys. 98 (2005) 044302.
[13] E. Tanabe, Y. Kitano, K. Yamada, M. Miyamoto, Y. Ohtani, S. Orimo, T. Ichikawa, H. Fujii, J. Japan Inst. Metals 69 (2005) 113–120.
[14] K. Tatsumi, S. Muto, T. Yoshida, J. Appl. Phys. 101 (2007) 023523.
[15] T. Kimura, S. Muto, K. Tatsumi, T. Tanabe, T. Kiyobayashi, J. Alloys Compd. 413 (2006) 150–154.
[16] C.I. Smith, H. Miyaoka, T. Ichikawa, M.O. Jones, J. Harmer, W. Ishida, P.P. Edwards, Y. Kojima, H. Fuji, J. Phys. Chem. C 113 (2009) 5409–5416.
[17] A. Oberlin, J.P. Rouchy, C. R. Acad. Sci. Paris Sci. Série C 268 (1969) 660–663.
[18] A. Oberlin, Carbon 9 (1971) 39.
[19] A. Oya, S. Otani, Carbon 17 (1979) 131–137.
[20] J.P. Huo, H.H. Song, X.H. Chen, S.Q. Zhao, C.M. Xu, Mater. Chem. Phys. 101 (2007) 221–227.
[21] K. Takai, R. Watanuki, ISIJ Int. 43 (2003) 520–526.